Chapter

CoMo/γ-Al_2O_3 Catalysts Prepared by Reverse Microemulsion: Synthesis and Characterization

José Luis Munguía-Guillén, José Antonio de los Reyes-Heredia, Michel Picquart, Marco Antonio Vera-Ramírez and Tomás Viveros-García

Abstract

A series of CoMo/γ-Al_2O_3 catalysts was synthesized by a reverse microemulsion method using 1-butanol as organic agent and cetyltrimethylammonium bromide as surfactant. The aqueous phase was used to form the solution of three corresponding Co, Mo and Al precursor salts. The materials were prepared at different solution concentrations in order to obtain different metal contents. All samples were characterized by X-ray diffraction, Raman spectroscopy, nuclear magnetic resonance and nitrogen physisorption. A chemical species distribution study was performed to establish conditions of preparation and the preponderant species present in solution as a function of pH. The materials obtained present high surface areas which decrease as the metal content (Co + Mo) increases. All samples with the exception of that with the highest metal content were amorphous as shown by X-ray diffraction. By Raman spectroscopy, Mo-O-Mo and MoO_{2t} species were observed in all calcined samples. Mo-O-Co, Al-O-Mo, monomers and heteropolymolybdates were observed for the lower metal content samples, and the formation of $CoMoO_4$ and aluminum molybdate species for the higher metal contents. These results suggest that the materials with lower metal loading have species that are easily sulfidable and provide high activity in hydrodesulfurization reactions. A model for the interaction of the species in the aqueous phase of the micelle is presented.

Keywords: reverse microemulsion, CoMo/γ-Al_2O_3 catalysts, chemical species distribution diagrams, catalyst characterization

1. Introduction

Regarding sulfur content in diesel fuels, more stringent environmental regulations have motivated research on new catalysts and novel synthesis methods, to produce highly active hydrodesulfurization (HDS) catalysts [1]. The commercial HDS catalysts are based on MoS_2 promoted by Co or Ni, supported on high-surface area γ-alumina. The most common synthesis procedure involves impregnation of aqueous solutions of Mo and Co (or Ni), followed by drying and calcination steps prior to the activation by a sulfur-containing agent. Generally, it is found that Mo could form a monolayer to prevent Ni or Co species to interact with the support. This

helps to avoid the formation of undesired species such as cobalt or nickel aluminates or segregated sulfides [2]. Nevertheless, different preparation sequences or procedures have been investigated since this is not a simple task [3, 4]. Furthermore, Co and Mo form the so-called "CoMoS" phase which has been reported as the active phase in this reaction to remove sulfur from compounds such as dibenzothiophene (DBT) and 4, 6-dimethyl dibenzothiophene (4,6-DMDBT) [4, 5]. This means to synthesize sulfides of 3 slabs stacking (CoMoS type II) [4, 6, 7]. It has also been reported that Co(Ni) MoS species can be obtained, with the use of thiomolybdate precursors in the presence of nonionic surfactants. Moreover, the morphology can be controlled, resulting in an increased activity as compared with more conventional synthesis using ammonium polymolybdates [8]. To carry out the impregnation of the support, solutions of ammonium heptamolybdate tetrahydrate and nickel(II) nitrate hexahydrate are generally used. Firstly, monomeric species such as MoO_4^{2-} are deposited on the carrier. These ions are obtained at pH values between 10 and 12 and MoO_3 species are formed after calcination [9, 10]. After impregnation of molybdenum, Co^{2+} species are impregnated at pH between 2 and 5.96 [11, 12] and CoO_x species are obtained after calcination [12]. Alternative synthesis methods have been tested. For instance, spray pyrolysis allowed the formation of nanosized spherical particles of CoMo sulfides supported on Al_2O_3 that increased the activity of the catalysts, due to weak interaction of CoMo and alumina [2].

A method capable of obtaining nanoparticles with interesting applications as heterogeneous catalysts is inverse microemulsion [13]. The water/oil microemulsion (reverse microemulsion) uses surfactant molecules to stabilize the water/oil interface of nanosized water droplets that are dispersed in an organic solvent. These water droplets consist of an aqueous solution of metal precursors [13, 14]. Recently, reverse microemulsion has been used to prepare NiMo catalysts by precipitation; after calcination and sulfidation, nickel was found decorating the edges of MoS_2. However, after HDS reaction, a significant amount of nickel was segregated, provoking a low activity in comparison with a NiMo/γ-Al_2O_3 catalyst taken as reference [15]. Reverse microemulsion is attractive to extend the actual studies to obtain CoMo/γ-Al_2O_3 catalysts with active species as required for HDS, preparing structured nanoparticles in only one step.

In the microemulsion systems, the interaction between ions in solution and the interface where the surfactant and the organic agent coexist is an important issue. ^{13}C NMR studies have shown that Co (II) is retained at the CTAB-hexanol-water interface, with a 1:1 interaction between Co(II) and hexanol [16]. Also, at low concentrations, octahedral Co(II) complexes are formed. On the other hand, in the preparation of alumina, sodium dodecyl sulfate (SDS, anionic) and cetyltrimethylammonium bromide (CTAB, cationic) have been used as mixtures in different proportions. It was found that the SDS head remains in the alumina network with a decrease in its surface area [17]. Some reports describe the synthesis of unsupported Co(Ni)-Mo-S catalyts for HDS reactions, using surfactants and chelating agents as textural promoters, and the materials obtained show bigger surface areas and a higher catalytic activity than commercial catalysts [8].

The effect of the surfactant on the preparation of CoMo/γ-Al_2O_3 by the microemulsion method was reported [18]. Sodium dodecyl sulfate (SDS) and cetyltrimethylammonium bromide (CTAB) were used and compared. Microemulsions synthesized with SDS provided larger size nanodrops than those obtained with CTAB, with a lower amount of surfactant added. After calcination, the solids prepared with SDS showed the presence of sodium sulfate and had surface areas 50% lower than those obtained with CTAB.

In this work, the preparation of catalysts by a reverse microemulsion method has been undertaken to provide nanostructured-supported metals used in HDS. A

series of CoMo/γ-Al_2O_3 catalysts were synthesized and characterized, and the influence of concentration of metals on the calcined solid materials was evaluated. In order to determine the solution conditions to obtain Co and Mo on Al_2O_3, chemical species distribution calculations were made. These calculations allowed us to establish pH and concentrations to employ for the microemulsion preparation and the proper chemical species to be obtained in the solid materials. In a first attempt to correlate the catalyst synthesis parameters with the resultant structural and textural characteristics, characterization of the oxidic phases by atomic absorption, N_2 physisorption, X-ray diffraction (XRD), magic angle spinning-nuclear magnetic resonance (MAS-NMR) and Raman spectroscopy is presented and discussed.

2. Experiment

2.1 Preparation of reverse microemulsions

Five samples were prepared using 1-butanol, water and cetyltrimethylammonium bromide (CTAB), according to the mass percentages shown in **Table 1**. All chemicals were reagent grade from Sigma Aldrich, otherwise it is indicated. **Figure 1** shows a diagram for material synthesis. For each catalyst, the organic phase was 1-butanol (C_4H_9OH), and the aqueous phase was composed of cobalt nitrate ($Co(NO_3)_2\ 6H_2O$), ammonium heptamolybdate (AHM, $(NH_4)_6Mo_7O_{24}\ 4H_2O$) and aluminum nitrate $Al(NO_3)_3\ 9H_2O$ (J. T. Baker). For each microemulsion, the required amount of CTAB ($CH_3(CH_2)_{15}NBr\ (CH_3)_3$) cationic surfactant was added. During the microemulsion formation, the mixture was continuously stirred with a magnetic stirrer, the CTAB surfactant was added slowly, until it turned from turbid to translucent. The electric conductivity was measured continuously with a LabPro Vernier (model CON-BTA) coupled to a conductivity probe with a sensitivity of ±0.001 S/m. Measurements were conducted at a constant temperature of 20 ± 0.1°C. Critical micelle concentration (cmc) was established for all the samples. This occurred at a point where the conductivity showed a sharp inflection point. Each microemulsion was adjusted to pH = 10 with n-butylamine to generate the required species in solution. Their molar concentrations are shown in the last three columns of **Table 1**. The use of pH 10 in the microemulsions was determined with the development of species distribution diagrams obtained through the Medusa (Make Equilibrium Diagrams Using Sophisticated Algorithms) program that generates distribution curves for species in solution, depicted as the logarithm of the concentration versus pH.

	Microemulsions			Species concentration		
Key	**Aqueous phase (%)**	**1-Butanol (%)**	**CTAB (%)**	**Co(II) (mM)**	**Mo(VI) (mM)**	**Al(III) (mM)**
C1	31.7	47.2	21.1	8.05	20.95	197.61
C2	31.9	47.4	20.7	8.50	22.14	162.43
C3	32.2	47.9	19.9	9.21	23.96	125.52
C4	32.6	48.4	19.0	9.65	25.11	78.95
C5	33.0	49.0	18.0	10.03	26.09	27.34

Table 1.
Nominal compositions for the synthesis of microemulsions.

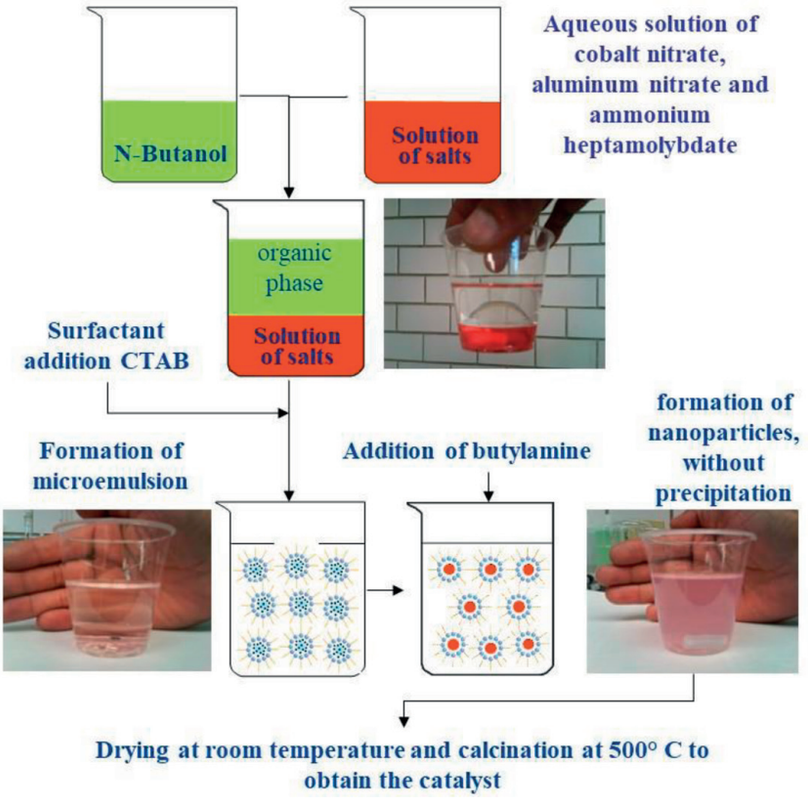

Figure 1.
Diagram for the synthesis method used for preparing the reverse microemulsion.

Subsequent to the formation of the microemulsions, the wet solids were maintained at room temperature for 48 h to evaporate the solvents. The obtained solids were calcined at 500°C for 6 h, with an air flow of 20 ml/min.

2.2 Characterization

The concentrations of the metallic elements in calcined samples were determined in a Varian SpectrAA 220 FS Atomic Absorption Spectrometer equipment. The spectrophotometer was calibrated with certified standards.

The nitrogen physisorption analysis for calcined catalysts was developed in an Autosorb 1 gas sorption system (Quantachrome). Samples were outgassed at 477 K under vacuum for 6 h. Then, nitrogen physisorption experiments were carried out at 77 K. The determination of surface area and volume and pore diameter were carried out using the BET equation and the BJH method, respectively.

To determine the coordination number and crystallographic arrangements of the synthesized support (alumina), a magic angle spinning-nuclear magnetic resonance equipment (MAS-NMR) Bruker Avance II 300, equipped with a multinuclear detector of 4-mm CPMAS with a frequency range ^{31}P to ^{15}N was utilized. Analyses were carried out with a rotational speed of 10 kHz.

The crystalline phases of the calcined samples were identified using a Siemens D-500 Kristalloflex diffractometer, with a CuKα radiation, λ = 0.15406 nm, and with primary and secondary monochromators. The equipment was operated at 35 kV, 20 mA, with a time interval of 1 s and scan rate of 0.03°/s.

Raman spectra for the calcined samples were recorded using Raman HORIBA Jobin Yvon T64000 equipment. The excitation laser source wavelength was 532.1 nm, with a power of 20 mW at the laser head; 100 scans of each sample were performed and accumulated at room temperature, and the spectra were recorded in the range 100–1300 cm^{-1}.

3. Results and discussion

3.1 Determination of species in solution

Figure 2 shows the theoretical diagrams for Co, Mo and Al species as determined from the MEDUSA program for the C3 CoMo/Al_2O_3 sample. A total of 28 possible reactions were considered, including 5 soluble compounds (H^+, Co^{2+}, MoO_4^{2-}, Al^{3+}, $C_4H_9NH_2$), 3 solid species ($Al(OH)_3$(cr), $Co(OH)_2$(c), H_2MoO_4(c)), and the other species were Co, Mo or Al complexes.

Figure 2a depicts the distribution of two Co species. One Co^{2+} species appeared at acidic pH and it decreased after a pH value higher than 7. At this value, the formation of $Co(OH)_2$ began to increase, reaching maximum concentration at pH higher than 8.5. Some authors have reported cobalt species in solution pH values higher than 6 [19, 20], in agreement with theoretical calculations. Moreover, these compounds exhibited also high stability.

Seven Mo species were identified in **Figure 2b**. Six of them were observed at acidic pH, among them $HMoO^{4-}$ y $Mo_7O_{24}^{6-}$ species were found at pH values between 4 and 6. MoO_4^{2-} species began to be noticeable at pH values around 4, reaching maximum concentration at pH higher than 6. Furthermore, this was the only remaining species at pH higher than 8. Regarding MoO_4^{2-} species, it has been reported that they exist primarily at low concentrations and at pH = 10 [11]. $[MoO_4]^{2-}$ has also been determined as the predominant oxo-molybdenum (VI) species in the catalyst MoO_3/Al_2O_3, in which case this species is found in solution and adsorbed on the alumina surface depending on the concentration of Mo [21–23].

Regarding Al, **Figure 2c** shows three species. Al^{3+} ions began to disappear at pH values near 2.8 and $Al(OH)_3$ concentration increased. This crystalline species reached its maximum concentration at pH = 4.3 and it decreased at pH = 10.5. The $Al(OH)_4^-$ species began to appear at pH = 11 and its concentration reached a maximum value at pH = 13.7.

Several authors have reported that $Al(OH)_3$ in solution was obtained at pH values between 8 and 11 [17, 24].

Table 2 gives those reactions favoring the most common complexes involved in CoMo catalysts synthesis. These were formed at pH 10. The results from reactions in **Table 2** were considered to establish concentration and pH ranges in which the formation of suitable species within the nanodroplets of the microemulsion may occur. Moreover, these values were taken into account to avoid the release and precipitation of solid particles. This can be observed when an excessive growth of particles within of the micelles takes place. For catalysts with different metal loading (C1, C2 C4 and C5 samples), analogous diagrams were obtained, showing the same species distribution.

Overall, the selected species to be obtained at the conditions fixed experimentally have been those needed for the formation of the precursors of the active species in HDS catalysts [9, 19, 20, 25].

3.2 Atomic absorption

Table 3 gives the results for metallic loadings as determined by atomic absorption for catalysts after calcination. According to **Table 3**, it can be observed that the Co/Mo ratio was around 0.236 for all the samples. Therefore, it was shown that the method of reverse microemulsion allowed us to obtain a Co/Mo ratio with the same average value for all samples, independently of the metal content. Furthermore, the ratio Co/Mo is comparable to metal contents in an industrial catalyst (CoMoind), taken as reference.

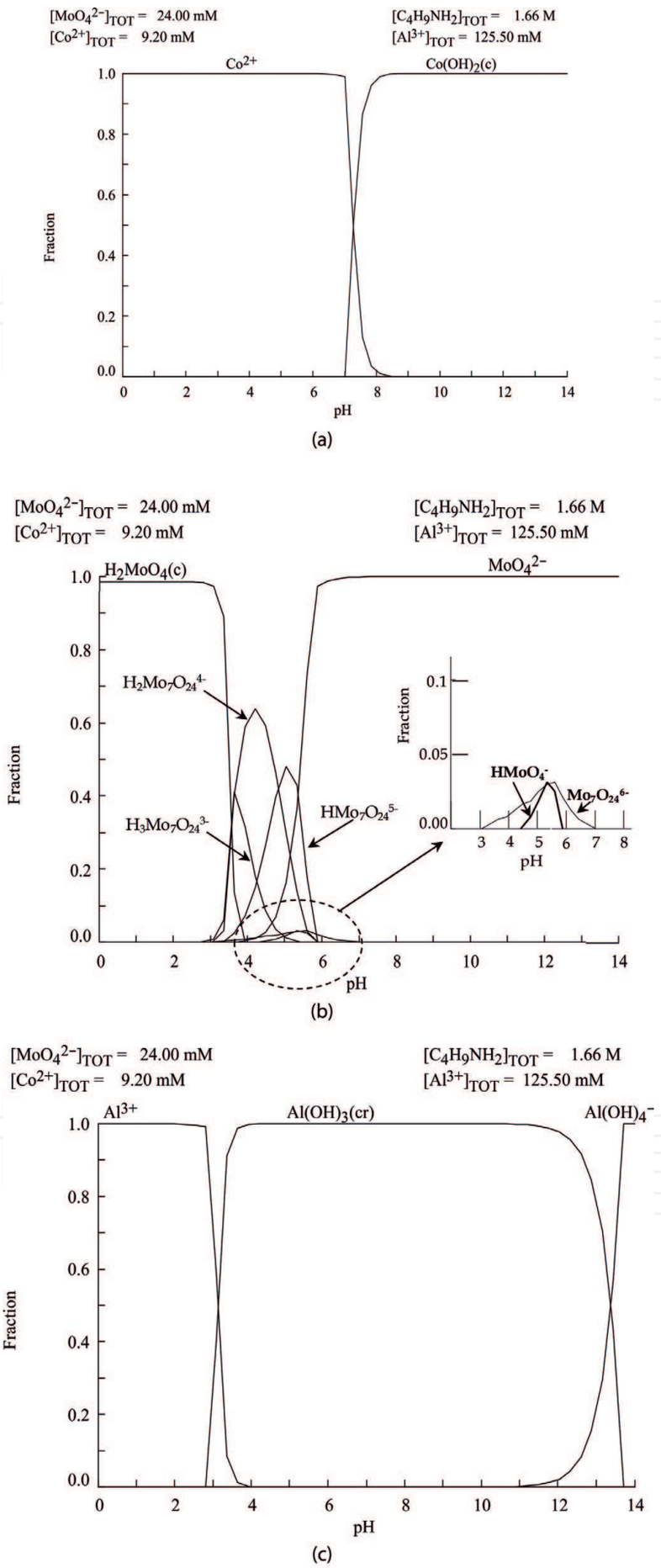

Figure 2.
Species distribution diagrams for the synthesis for CoMo/γ-Al_2O_3 catalysts (C3): (a) cobalt species, (b) molybdenum species (c), aluminum species.

Ions		Formed species	log K
$2H_2O + Co^{2+}$	=	$2H^+ + Co(OH)_{2\,(c)}$	−18.6
$3H_2O + Al^{3+}$	=	$3H^+ + Al(OH)_{3(cr)}$	−8.11
$4H_2O + Mo_7O_{24}^{6-}$	=	$8H^+ + 7MoO_4^{2-}$	−52.99

Table 2.
Hydrolysis reactions for Al, Co and Mo species.

CoMo/γ-Al_2O_3 catalysts have been synthesized by several methods and previous papers [4] agree that the content of metals on the support, including an average ratio of Co/Mo of 0.24, is adequate to prepare active HDS catalysts. However, it has also been reported that metal loading on the support depends on the method of preparation [4]. In some cases, it has been determined that the number of slabs on the support (alumina) increases and the edges on the slabs decrease with increasing Mo content. These edges are generally decorated by deposition of cobalt species as promoter [7]. Therefore, the metal loading must be controlled to an extent, that is, 15 or 20 wt.% of Mo, since high loadings lead to the formation of inactive structures [4]. Furthermore, some studies have been aimed at obtaining a monolayer of molybdenum species on the surface of the carrier and Co/(Co + Mo) ratios corresponding to high dispersion of Co on the edges of the slabs of molybdenum [25, 26]. In our case, the results indicate that precipitation of the particles out of the micelles of the microemulsion systems did not occur during catalyst preparation, since it would have resulted in a heterogeneous distribution of the catalyst composition.

3.3 Nitrogen physisorption

Results for nitrogen physisorption for the catalysts in this work and for an industrial catalyst are given in **Table 4**. Catalysts C1, C2 and C3 exhibited higher surface areas than the industrial catalyst (CoMoind). Catalyst C4 showed a comparable surface area as that of the CoMoind sample, while the C5 catalyst exhibited a significantly lower surface area. Furthermore, pore diameter values increased from catalyst C1 to C5, showing a comparable value between C2 and CoMoind. One of the fundamental aspects of the analysis of physisorption that has been suggested for HDS supports is that their surface area must be high enough to ensure a high dispersion of the active species [2].

Thus, we observed high surface areas for the synthesized catalysts by using microemulsions. It is possible that nanosized particles were formed inside the micelles systems as reported in the literature [27–30]. However, high Mo loading such as those in C4 and C5 catalysts could lead to different porous structures and one cannot rule out pore blocking by the metals.

Key	Co (wt.%)	Mo (wt.%)	Co/Mo
C1	3.7	15.3	0.236
C2	4.6	18.6	0.234
C3	5.6	24.0	0.238
C4	8.0	33.1	0.238
C5	13.2	54.6	0.235
CoMoind	5.7	24.5	0.233

Table 3.
Metal content for the catalysts as determined by atomic absorption.

3.4 Spinning-nuclear magnetic resonance equipment (MAS-NMR)

Figure 3 shows the ^{27}Al MAS-NMR spectrum for the C3 catalyst before calcination. One can observe a broad band with a maximum at around 0 ppm, that can be ascribed to the formation of the $Al(OH)_3$ (gibbsite) compound. This species has low electronegativity and, therefore, it can interact more easily with more electronegative elements [31], such as molybdenum species, rather than with cobalt species. This is relevant for the preparation method, considering that the latter has a tendency to form cobalt aluminate with the support when using impregnation methods [3, 32, 33].

Figure 4 displays the ^{27}Al MAS-NMR spectra for the calcined catalysts. The CoMoind sample exhibited a broad band at 0 ppm that can be assigned to octahedral species of the support. Besides, formation of tetrahedral species was determined as a weak band at around 60 ppm. These two bands are characteristic of γ-Al_2O_3 [34, 35]. It is likely that during calcination up to 250°C, the gibbsite formed boehmite (α-AlO(OH)). This compound was transformed to γ-Al_2O_3, when the temperature reached 500°C [36].

Additionally, **Figure 4** shows that pentahedral species between 40 and 50 ppm appeared for the C5 and CoMoind catalysts. These species have been identified as defects in the support structure, as originated by the replacement of oxygen in the network of octahedral symmetry by hydroxyl groups [37]. For C5 sample, a band around −14 ppm was detected. This band has been related to the presence of the $Al_2(MoO_4)_3$ species which distorts the octahedral network of the support [35].

Some authors have reported that the $Al_2(MoO_4)_3$ species can be due to the dissolution of the Al^{3+} species, which subsequently react with heptamolybdate complexes during the impregnation step, forming the Anderson-type heteropolymolybdate $[Al(OH)_6Mo_6O_{18}]^{3-}$ [35]. In this study, the appearance of the molybdate species (around −15 ppm) could be due to the formation of an Anderson-type heteropolymolybdate obtained in the synthesis mixture.

3.5 X-ray diffraction

Figures 5 and **6** show the diffractograms for the calcined catalysts. As it can be seen, no XRD lines were observed for almost all catalysts, except for the C5 solid, pointing out to amorphous solids. Thus, cobalt and molybdenum oxides may be highly dispersed on the support (γ-Al_2O_3). This has also been observed by other authors who detected a broad band between 5 and 50° (2Θ) describing amorphous catalysts. **Figure 6** (extended from **Figure 5**) shows the diffractogram for the C5 catalyst. Well-defined XRD lines were detected and they were associated with $CoMoO_4$ and $Al_2(MoO_4)_3$ [2]. This finding is consistent with MAS-RMN results for the highly loaded CoMo catalyst (C5).

Catalysts Tc (500°C)	S_{BET} (m^2/g)	Pore volume (cm^3/g)	D_p (Å)
C1	294	0.74	55.8
C2	286	0.62	56.2
C3	261	0.41	68.3
C4	212	0.28	71.2
C5	125	0.19	76.2
CoMoind	204	0.49	56.6

Table 4.
Nitrogen physisorption results for the calcined catalysts.

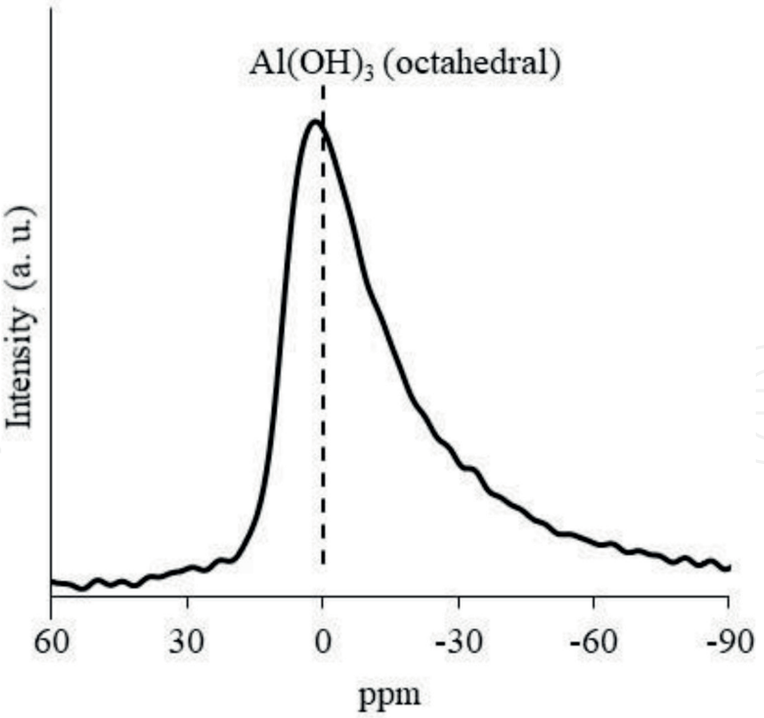

Figure 3.
^{27}Al MAS-NMR spectrum for the C3 CoMo/γ-Al_2O_3 uncalcined catalyst.

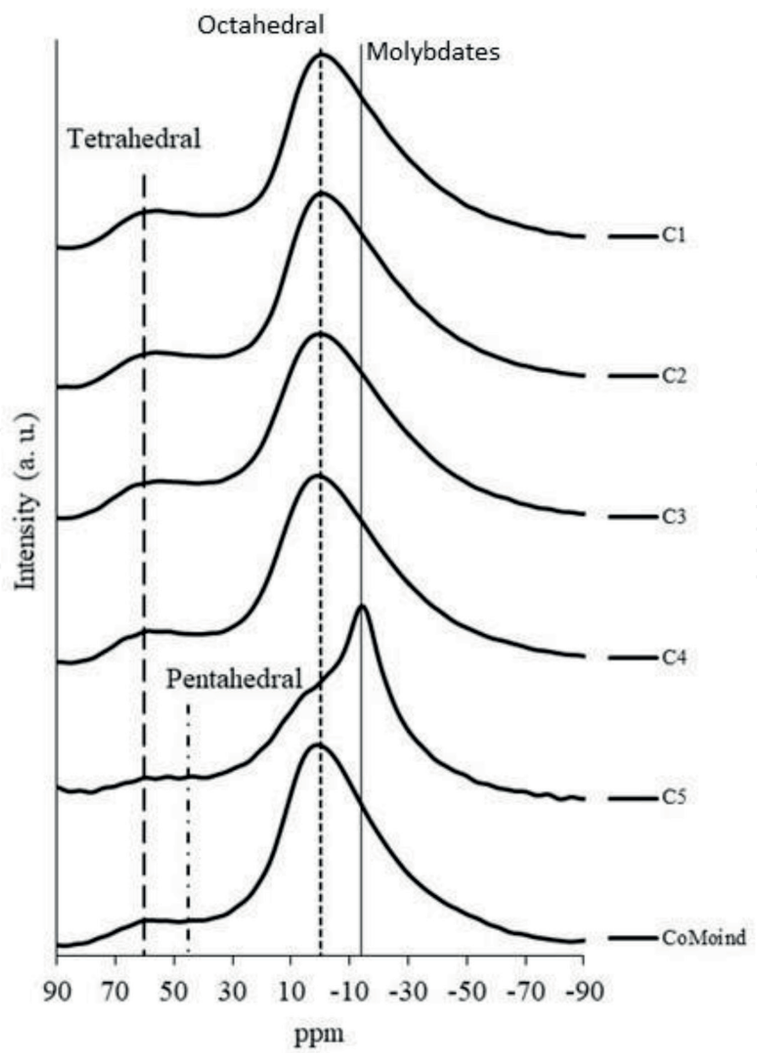

Figure 4.
^{27}Al MAS-NMR spectra for the CoMo/γ-Al_2O_3 calcined catalysts series.

3.6 Raman analysis

Raman spectra for the CoMo/γ-Al_2O_3 catalysts series and the CoMoind catalyst are given in **Figure 7**. For C1, C2 and C3 CoMo catalysts, more attenuated and wider bands were observed, as compared with C4 and C5 spectra. It could be due to more microcrystalline particles in low-content Mo samples. Thus, particle sizes for highly loaded catalysts C4 and C5 were larger, as expected.

Table 5 summarizes all the Raman bands indicating the type of species as assigned for the catalysts in oxidic state. To assign the species present in the samples, the signals were deconvoluted and identified according to those reported in the literature.

One can notice bands between 500 and 700 cm^{-1} for C1 and C2 catalysts. These peaks can be assigned to the stretching mode vibration for bridged Mo-O-M links [38]. Specifically, the presence of Mo-O-Co bonds between 540 and 560 cm^{-1} was identified. This type of band corresponds to the interval of heteropolymolybdate structures and they indicate a strong interaction between cobalt and molybdenum oxides. This means that a weak interaction with the support occurs and, thus, it can induce a high degree of sulfidation of the catalyst as published by others [2, 39]. Besides, bands at 817–818 cm^{-1} were observed for samples with Mo loadings >20% in catalysts C4 and C5. These peaks are generated by MoO_3 species, indicating that a monolayer of MoO_3 on the surface of the support has been exceeded [40, 41]. Moreover, these MoOx species have been identified as orthorhombic molybdate species [42, 41]. Bands between 850 and 875 cm^{-1} were attributed to Mo-O-Mo bonds, assigned to the asymmetric vibrational stretching mode [2, 41, 43]. Other bands located between 930 and 960 cm^{-1} were assigned to Mo=O links, as the vibrational stretching mode for the dioxo groups in oxomolybdate species. This indicates the formation of MoO_{2t} species, where t indicates terminal oxygen atoms. This type of species was present in all studied catalysts, as tetrahedral MoOx structures on alumina [40].

Furthermore, it was found that the bands corresponding to the Mo-O-Mo links increased proportionally when increasing the bands corresponding to the MoO_{2t} links [2, 41, 43]. This suggests that there was an increase in the number of bridges of Mo, which implied high dispersion of Mo on the support [40, 44].

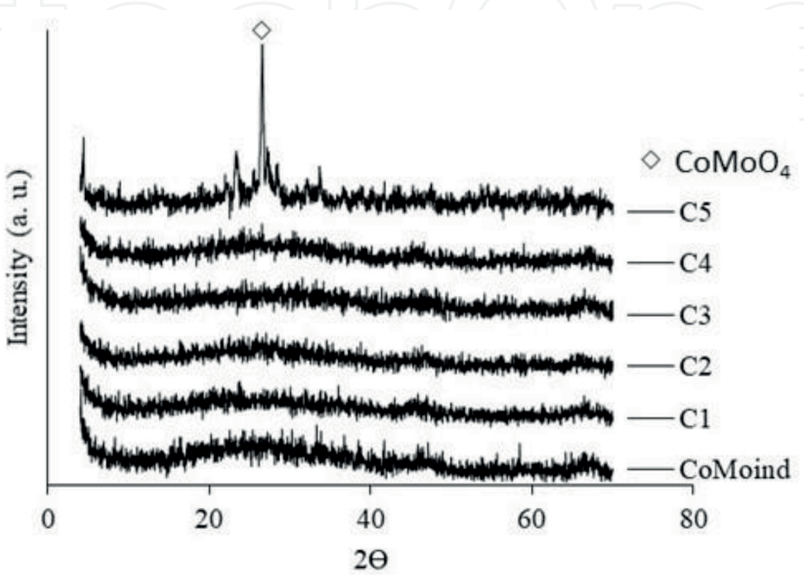

Figure 5.
XRD results for the CoMo/γ-Al_2O_3 calcined catalysts series.

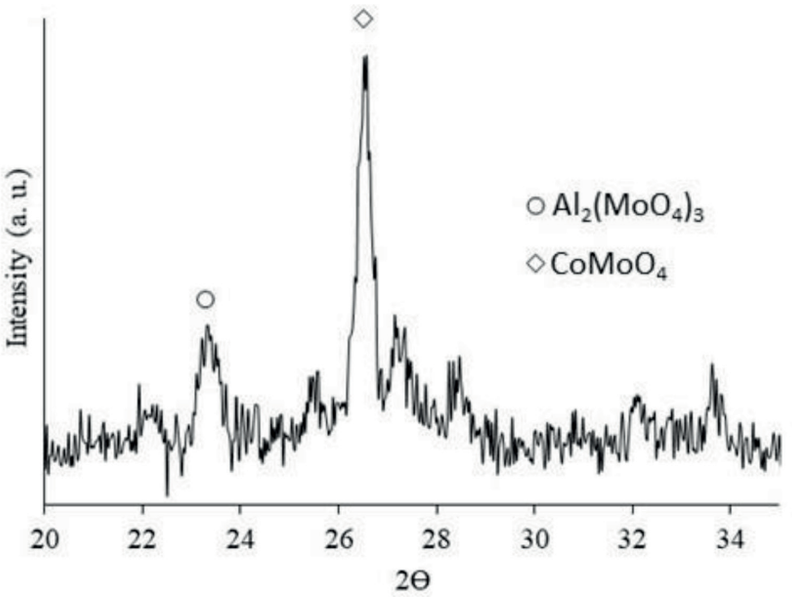

Figure 6.
XRD results for the CoMo/γ-Al_2O_3 calcined C5 catalyst.

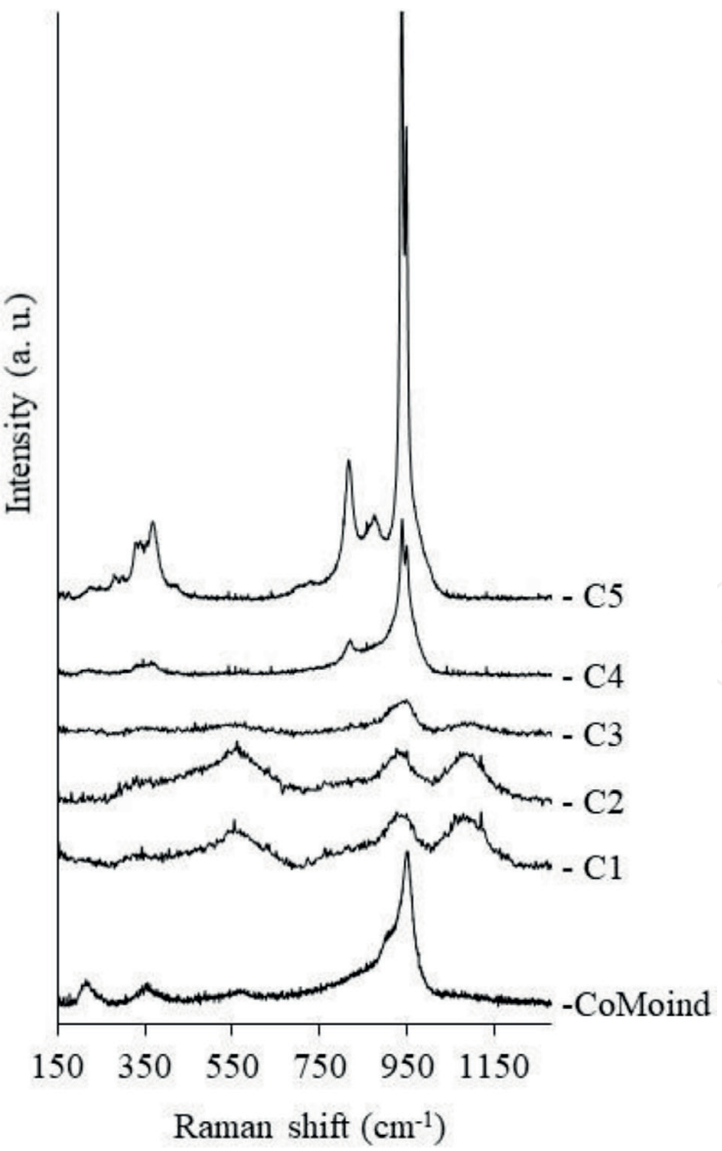

Figure 7.
Raman spectra for the CoMo/γ-Al_2O_3 calcined catalysts series.

Range (cm^{-1})	C1	C2	C3	C4	C5	CoMoind	Assigned species
200–300						215	Heptamolybdates or octamolybdates
300–400	320	320	360	335–365	346–369	354	Monomers Heptamolybdates or octamolybdates
500–700	570	570				560	Mo-O-Co Al-O-Mo
800–900	850	850	870	818 870	817 875	850	MoO_3 Mo-O-Mo
900–1000	937	930	930, 950	939, 950 978	905 938, 949 978	918 951	$CoMoO_4$ $*MoO_{2t}$ $Al_2(MoO_4)_3$
1000–1100	1085	1086	1090			1045	$(MoO_4)^{2-}$

Table 5.
Raman bands and the species associated for the calcined CoMo/γ-Al_2O_3 catalysts.

Additionally, bands between 905 and 918 cm^{-1} for the C5 and CoMoind catalysts were attributed to the presence of molybdate $CoMoO_4$ species, either isolated or polymerized, involving a strong interaction with the support. As reported by some authors [33, 42, 45, 46], the formation of aluminum molybdate species occurs at high Mo loadings. It has been published also that some amount of Mo reacts with Co during calcination.

For C1 and C2 catalysts, a band in the range between 970 and 1100 cm^{-1} was detected and highly dispersed MoO_4 tetrahedral species can be assigned in agreement with MAS-NMR results. It is likely that these metal loadings did not reach the MoOx monolayer formation [44, 47]. Moreover, the bands appearing between 200 and 400 cm^{-1} were attributed to Mo monomeric species [33].

Regarding Co species, no bands associated with this oxide were identified. However, since no segregation of Co species was noticed, one can propose that there exists an interaction of Mo and Co.

3.7 A model for the interaction of species in solution and the micelle

The results obtained in this work for the characterization of the catalytic materials demonstrate that these have: high surface areas, amorphous γ-Al_2O_3, a MoO_3 type species on the surface of the support and a constant Co/Mo ratio independent of the metal loading. Overall, it is possible to establish an interaction between Co species at the interface with the micelles, preventing the migration of Co into the alumina network. There is also an interaction between Mo and AlOOH in solution which hindered the Co-Al interaction and promoted the formation fo Mo-O-Co, as shown by Raman results. It is possible to depict a representative scheme of the species inside the micelles as can be observed in **Figure 8**. In this diagram, 1-butanol replaces water in the first coordination sphere of Co ion, so that Co is retained at the interface of the micelles [16].

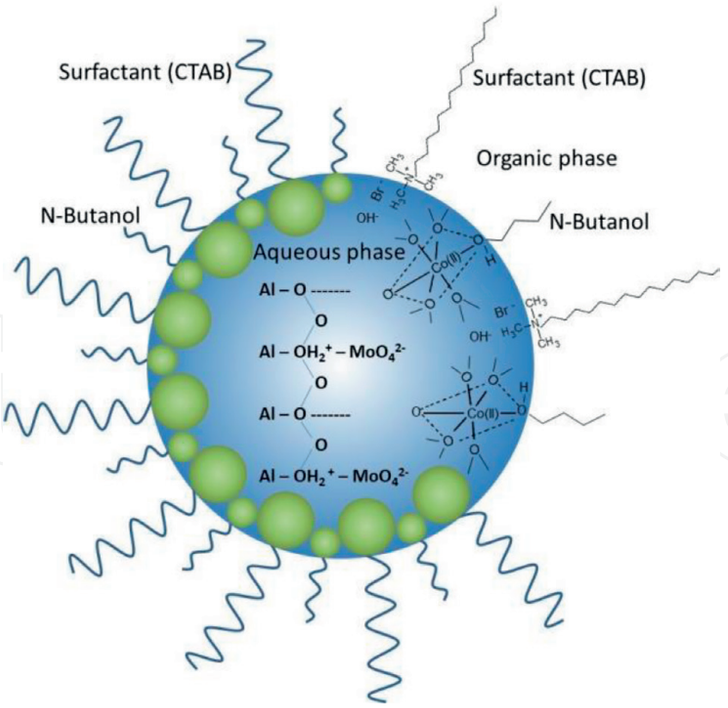

Figure 8.
Schematic diagram for the interaction between species in solution within the micelle. Al species interacting with Mo species, Co species located at the interface.

4. Conclusions

CoMo/γ-Al_2O_3 catalysts were synthesized at several metal (Co + Mo) contents employing a reverse microemulsion method. The microemulsion was formed using 1-butanol as organic agent, cetyltrimethylammonium bromide as surfactant and water. A study of chemical species distribution in solution as a function of pH was performed and provided the pH and precursor salt concentrations to be used in the synthesis to obtain the desired final material. The study allowed to obtain stable micelles, no precipitation of the metallic particles outside the micelles occurred and a constant Co/Mo ratio in all samples independent of the metal loading was observed. The solids calcined at 500°C showed large surface areas which decrease as the metal content was increased. All the calcined samples were amorphous for X-ray diffraction and only at the highest Co + Mo concentration some crystalline phases were found. On these samples, species such as Mo-O-Mo, MoO_{2t}, Mo-O-Co, Al-O-Mo were detected. These species are considered precursors of highly active catalytic sites in HDS reactions. Based on these results, a schematic model for the micelle formed was produced. In this model, Al and Mo species in solution interact whereas Co species interact with 1-butanol at the interface. With this model, it is possible to envisage the formation of the solid material with Mo covering the surface of Al_2O_3 and Co interacting with Mo on the surface of the aluminum oxide.

Acknowledgements

The authors would like to thank CONACYT-Mexico and UAM for the financial support. J. L. Munguía thanks CONACYT-Mexico for the scholarship granted.

Author details

José Luis Munguía-Guillén[1], José Antonio de los Reyes-Heredia[1], Michel Picquart[2], Marco Antonio Vera-Ramírez[3] and Tomás Viveros-García[1*]

1 Department of Process and Hydraulics Engineering, Basic Sciences and Engineering Division, Universidad Autónoma Metropolitana, Iztapalapa, Ciudad de México, México

2 Department of Physics, Basic Sciences and Engineering Division, Universidad Autónoma Metropolitana, Iztapalapa, Ciudad de México, México

3 Department of Chemistry, Basic Sciences and Engineering Division, Universidad Autónoma Metropolitana, Iztapalapa, Ciudad de México, México

*Address all correspondence to: tvig@xanum.uam.mx

References

[1] Babich IV, Moulijn JA. Science and technology of novel processes for deep desulfurization of oil refinery streams: A review. Fuel. 2003;**82**:607-631. DOI: 10.1016/s0016-2361(02)00324-1

[2] Choi K-H, Korai Y, Mochida I. Preparation and characterization of nano-sized CoMo/Al_2O_3 catalyst for hydrodesulfurization. Applied Catalysis A: General. 2004;**260**:229-236. DOI: 10.1016/j.apcata.2003.10.019

[3] Papadopoulou C, Vakros J, Matralis HK, Kordulis C, Lycourghiotis A. On the relationship between the preparation method and the physicochemical and catalitic properties of the CoMo/Al_2O_3 hydrodesulfurization catalysts. Journal of Colloid and Interface Science. 2003;**261**:146-153. DOI: 10.1016/s0021-9797(02)00167-4

[4] Topsoe H, Clausen BS, Massoth FE. Hydrotreating Catalysis, 1st ed. Berlin Heidelbergh: Springer-Verlag; 1996. 310 p. DOl: 10.1007/978-3-642-61040-0_1

[5] Choi KH, Kunisada N, Korai Y, Mochida I, Nakano K. Facile ultra-deep desulfurization of gas oil through two-stage or -layer catalyst bed. Catalysis Today. 2003;**86**:277-286. DOI: 10.1016/S0920-5861(03)00413-9

[6] Carlsson A, Brorson M, Topsoe H. Morphology of WS_2 nanoclusters in WS_2/C hydrodesulfurization catalysts revealed by high-angle annular dark-field scanning transmission electron microscopy (HAADF-STEM) imaging. Journal of Catalysis. 2004;**227**:530-536. DOI: 10.1016/j.jcat.2004.08.031

[7] Lauritsen JV, Nyberg M, Norskov JK, Clausen BS, Topsoe H, Laegsgaard E, et al. Hydrodesulfurization reaction pathways on MoS_2 nanoclusters revealed by scanning tunneling microscopy. Journal of Catalysis. 2004;**224**:94-106. DOI: 10.1016/j.jcat.2004.02.009

[8] Genuit D, Afanasiev P, Vrinat M. Solution syntheses of unsupported Co(Ni)–Mo–S hydrotreating catalysts. Journal of Catalysis. 2005;**235**:302-317. DOI: 10.1016/j.jcat.2005.08.016

[9] Spanos N, Vordonis L, Kordulis C, Lycourghiotis A. Molybdenum-oxo species deposited on alumina by adsorption: I. Mechanism of the adsorption. Journal of Catalysis. 1990;**124**:301-314. DOI: 10.1016/0021-9517(90)90179-n

[10] Wang L, Hall WK. The preparation and genesis of molybdena-alumina and related catalyst systems. Journal of Catalysis. 1982;**77**:232-241. DOI: 10.1016/0021-9517(82)90163-4

[11] Bergwerff JA, Visser T, Weckhuysen BM. On the interaction between Co- and Mo-complexes in impregnation solutions used for the preparation of Al_2O_3-supported HDS catalysts: A combined Raman/UV-vis-NIR spectroscopy study. Catalysis Today. 2008;**130**:117-125. DOI: 10.1016/j.cattod.2007.06.037

[12] Vakros J, Papadopoulou C, Voyiatzis GA, Lycourghiotis A, Kordulis C. Modification of the preparation procedure for increasing the hydrodesulfurisation activity of the CoMo/γ-Al_2O_3 catalysts. Catalysis Today. 2007;**127**:85-91. DOI: 10.1016/j.cattod.2007.02.028

[13] Eriksson S, Nylén U, Rojas S, Boutonnet M. Preparation of catalysts from microemulsions and their applications in heterogeneous catalysis. Applied Catalysis A: General. 2004;**265**:207-219. DOI: 10.1016/j.apcata.2004.01.014

[14] Uskokovic V, Drofenik M. Synthesis of materials within reverse micelles. Surface Review and Letters.

2005;**12**:239-277. DOI: 10.1142/S0218625X05007001

[15] Scott CE, Pérez-Zurita MJ, Carbognani LA, Molero H, Vitale G, Guzman HJ, et al. Preparation of NiMoS nanoparticles for hydrotreating. Catalysis Today. 2015;**250**:21-27. DOI: 10.1016/j.cattod.2014.07.033

[16] Nagy JB. Preparation of ultrafine particles of metals and metal borides in microemulsions. In: Kumar P, Mittal KL, editors. Handbook of Microemulsion Science and Technology. 1st ed. New York: Marcel Dekker AG; 1999. pp. 499-547. ISBN: 0-8247-1979-4

[17] Sicard L, Lebeau B, Patarin J, Kolenda F. Synthesis of mesostructured or mesoporous aluminas in the presence of surfactants. Comprehension of the mechanisms of formation. Oil & Gas Science and Technology. 2003;**58**:557-569. DOI: 10.2516/ogst:2003039

[18] Munguía-Guillén JL, Vernon-Carter EJ, De los Reyes-Heredia JA, Viveros-García T. Effect of surfactant in the synthesis of $CoMo/Al_2O_3$ catalysts obtained by reverse microemulsion for dibenzothiophene hydrodesulfurization. Revista Mexicana de Ingeniería Química. 2016;**15**:893-902. ISSN electronic: 2395-8472

[19] Vakros J, Bourikas K, Kordulis C, Lycourghiotis A. Structure of Co(II) species formed on the surface of γ-alumina upon interfacial deposition. The Open Catalysis Journal. 2014;**7**:8-17. DOI: 10.2174/1876214X01407010008

[20] Towle SN, Bargar JR, Brown GE, Parks GA. Surface precipitation of Co (II)(aq) on Al_2O_3. Journal of Colloid and Interface Science. 1997;**187**:62-82. DOI: 10.1006/jcis.1996.4539

[21] Blanchard P, Mauchausse C, Payen E, Grimblot J, Poulet O, Boisdron N, et al. Preparation and characterization of $CoMo/Al_2O_3$ HDS catalysts: Effects of a complexing agent. Studies in Surface Science and Catalysis. 1995;**91**:1037-1049. DOI: 10.1016/s0167-2991(06)81847-1

[22] Blanchard P, Lamonier C, Griboval A, Payen E. New insight in the preparation of alumina supported hydrotreatment oxidic precursors: A molecular approach. Applied Catalysis, A: General. 2007;**322**:33-45. DOI: 10.1016/j.apcata.2007.01.018

[23] Iannibello A, Mitchell PCH. Preparative chemistry of cobalt-molibdenum/alumina catalysts. Studies in Surface Science and Catalysis. 1979;**3**:469-478. DOI: 10.1016/s0167-2991(09)60230-5

[24] Parida KM, Pradhan AC, Das J, Sahu N. Synthesis and characterization of nano-sized porous gamma-alumina by control precipitation method. Materials Chemistry and Physics. 2009;**113**:244-248. DOI: 10.1016/j.matchemphys.2008.07.076

[25] Bezverkhyy I, Afanasiev P, Lacroix M. Promotion of highly loaded MoS_2/Al_2O_3 hydrodesulfurization catalysts prepared in aqueous solution. Journal of Catalysis. 2005;**230**:133-139. DOI: 10.1016/j.jcat.2004.12.009

[26] Pérez De la Rosa M, Texier S, Berhault G, Camacho A, Yacamán MJ, Mehta A, et al. Structural studies of catalytically satabilized model and industrial-supported hydrodesulfurization catalysts. Journal of Catalysis. 2004;**225**:288-299. DOI: 10.1016/s0021-9517(04)00161-7

[27] Corolleur C, Tomanova D, Gault FG. The mechanisms of hydrogenolysis and isomerization of hydrocarbons on metals: VII. Isomerization of labeled hexanes and hydrogenolysis of methyl (^{13}C) cyclopentane on a 10% platinum-alumina catalyst. Journal of Catalysis. 1972;**24**:401-416. DOI: 10.1016/0021-9517(72)90124-8

[28] Boutonnet M, Kizling J, Mintsa-Eya V, Choplin A, Touroude R, Maire G, et al. Monodisperse colloidal metal particles from nonaqueous solutions: Catalytic behavior in hydrogenation of but-1-ene of platinum, palladium, and rhodium particles supported on pumice. Journal of Catalysis. 1987;**103**:95-104. DOI: 10.1016/0021-9517(87)90096-0

[29] Dutta P, Fendler JH. Preparation of cadmium sulfide nanoparticles in self-reproducing reversed micelles. Journal of Colloid and Interface Science. 2002;**247**:47-53. DOI: 10.1006/jcis.2001.8097

[30] Hayashi H, Chen LZ, Tago T, Kishida M, Wakabayashi K. Catalytic properties of Fe/SiO_2 catalysts prepared using microemulsion for CO hydrogenation. Applied Catalysis A: General. 2002;**231**:81-89. DOI: 10.1016/s0926-860x(01)00948-6

[31] Hu Y, Liu X, Xu Z. Role of cristal structure in flotation separation of diaspore from kaolinite, pyrophyllite and illite. Minerals Engineering. 2003;**16**:219-227. DOI: 10.1016/s0892-6875(02)00368-0

[32] Liu F, Xu S, Cao L, Chi Y, Zhang T, Xue D. A comparison of $NiMo/Al_2O_3$ catalysts prepared by impregnation and coprecipitation methods for hydrodesulfurization of dibenzothiophene. Journal of Physical Chemistry C. 2007;**111**:7396-7402. DOI: 10.1021/jp068482+

[33] Papadopoulou C, Vakros J, Matralis HK, Voyiatzis GA, Kordulis C. Preparation, characterization, and catalytic activity of $CoMo/Al_2O_3$ catalysts prepared by equilibrium deposition filtration and conventional impregnation techniques. Journal of Colloid and Interface Science. 2004;**274**:159-166. DOI: 10.1016/j.jcis.2003.11.041

[34] Escobar J, De Los Reyes JA, Viveros T. Sol-gel Al_2O_3 structure modification by Ti and Zr addition. A NMR study. Studies in Surface Science and Catalysis. 2000;**143**:547-554. DOI: 10.1016/S0167-2991(00)80696-5

[35] Klimova T. Concerning the interpretation of ^{27}Al MAS-NMR spectra of Mo and NiMo catalysts on Al-containing MCM-41 supports: A reply to the comment by X. Carrier and M. Che on "Ni and Mo interaction with Al-containing MCM-41 support and its effect on the catalytic behavior in DBT hydrodesulfurization" [Appl. Catal. A 240 (2003) 29-40]. Applied Catalysis A: General. 2003;**253**:321-325. DOI: 10.1016/s0926-860x(03)00504-0

[36] Digne M, Sautet P, Raybaud P, Toulhoat H, Artacho E. Structure and stability of aluminum hydroxides: A theoretical study. The Journal of Physical Chemistry B. 2002;**106**: 5155-5162. DOI: 10.1021/jp014182a

[37] Wang JA, Bokhimi X, Morales A, Novaro O. Aluminum local environment and defects in the crystalline structure of sol–gel alumina catalyst. The Journal of Physical Chemistry B. 1999;**103**(2): 299-303. DOI: 10.1021/jp983130r

[38] Cabello CI, Muñoz M, Payen E, Thomas HJ. Influence of cobalt content on the hydrotreatment catalytic activity of $CoMo_6/\gamma\text{-}Al_2O_3$ heteropolyoxomolybdate-based catalyst. Catalysis Letters. 2004;**92**:69-73. DOI: 10.1023/B:CATL.0000011090.71716.6e

[39] Escobar J, Toledo JA, Cortés MA, Mosqueira ML, Pérez V, Ferrat G, et al. Highly active sulfided CoMo catalysts on nano-structured TiO_2. Catalysis Today. 2005;**106**:222-226. DOI: 10.1016/j.cattod.2005.07.136

[40] Dzwigaj S, Louis C, Breysse M, Cattenot M, Belliere V, Geantet C, et al. New generation of titanium dioxide support for hydrodesulfurization. Applied Catalysis B: Environmental. 2003;**41**:181-191. DOI: 10.1016/s0926-3373(02)00210-2

[41] Vuurman MA, Wachs IE. In situ Raman spectroscopy of alumina-supported metal oxide catalysts. The Journal of Physical Chemistry. 1992;**96**:5008-5016. DOI: 10.1021/j100191a051

[42] Guevara-Lara A, Bacaud R, Vrinat M. Highly active NiMo/TiO_2-Al_2O_3 catalysts: Influence of the preparation and the activation conditions on the catalytic activity. Applied Catalysis A: General. 2007;**328**:99-108. DOI: 10.1016/j.apcata.2007.05.028

[43] Christodoulakis A, Heracleous E, Lemonidou AA, Boghosian S. An operando RAMAN study of structure and reactivity of alumina-supported molybdenum oxide catalysts for the oxidative dehydrogenation of ethane. Journal of Catalysis. 2006;**242**:16-25. DOI: 10.1016/j.jcat.2006.05.024

[44] Mojet BL, Coulier L, van Grondelle J, Niemantsverdriet JW, van Santen RA. Potential of UV-RAMAN spectroscopy for characterization of sub-monolayer MoOx model catalysts at ambient pressure. Catalysis Letters. 2004;**96**:1-4. DOI: 10.1023/B:CATL.0000029521.80714.8d

[45] Jia M, Afanasiev P, Vrinat M. The influence of preparation method on the properties of NiMo sulfide catalysts supported on ZrO_2. Applied Catalysis A: General. 2005;**278**:213-221. DOI: 10.1016/j.apcata.2004.09.037

[46] Mazurelle J, Lamonier C, Lancelot C, Edmond P, Pichon C, Guillaume D. Use of the cobalt salt of the heteropolyanion $[Co_2Mo_{10}O_{38}H_4]^{6-}$ for the preparation of CoMo HDS catalysts supported on Al_2O_3, TiO_2 and ZrO_2. Catalysis Today. 2008;**130**:41-49. DOI: 10.1016/j.cattod.2007.07.008

[47] Haber J. Molybdenum compounds in heterogeneous catalysis. In: Braithwaite ER, Haber J, editors. Molybdenum: An Outline of its Chemistry and Uses. 1st ed. Amsterdam: Elsevier Science; 1994. pp. 477-617. ISBN: 9781483290898